DIFFUSION, WAVES, PHASE AND EDDY

CURRENT IMAGING

L. Udpa and W. Lord

Electrical Engineering Department
Colorado State University
Fort Collins, CO 80523

INTRODUCTION

The discovery of electromagnetic induction by Faraday and Henry in 1831 not only served as the catalyst needed for the very creation of electrical engineering but also provided the physical basis for eddy current nondestructive testing (NDT) as we know it today and as first realized in the classical experiments of Hughes[1] . As this fundamental work preceded Maxwell's prediction of electromagnetic wave phenomena by over half a century, it may seem somewhat surprising to the casual reader that there should be any need to explain why eddy current NDT phenomena can be classified as quasi-static in nature with none of the attributes of classical electromagnetic waves. Unfortunately, there are many misconceptions concerning the wave-like nature of eddy current NDT phenomena which have even led to the suggestion[2] that conventional eddy current NDT probe signals can be treated holographically. There are several reasons for the existence of these misconceptions:

1.   Many papers in the field (see for example Hochschild[3]) describe the propagation of an electromagnetic plane wave in a medium as being analogous to eddy current NDT phenomena. Although the analog itself has some limited validity, it is rarely if ever mentioned that a conventional eddy current NDT probe does not launch an electromagnetic wave (as does say an antenna).

2.   Solution of the quasi-static skin effect equation for current density does have the same form as would a damped electromagnetic wave. However, this is more a statement of the consistency of Maxwell's equations across different regimes (see Figure 1) than support for eddy current waves. A number of authors address this seemingly anomalous situation (see for example, Stoll[4] , Ferrari[5] , and Melcher[6]) and clearly differentiate between electromagnetic diffusion and electromagnetic wave phenomena.

3.   Much of the terminology associated with eddy current NDT phenomena (phase, for example) has a direct counterpart in electromagnetic wave parlance.
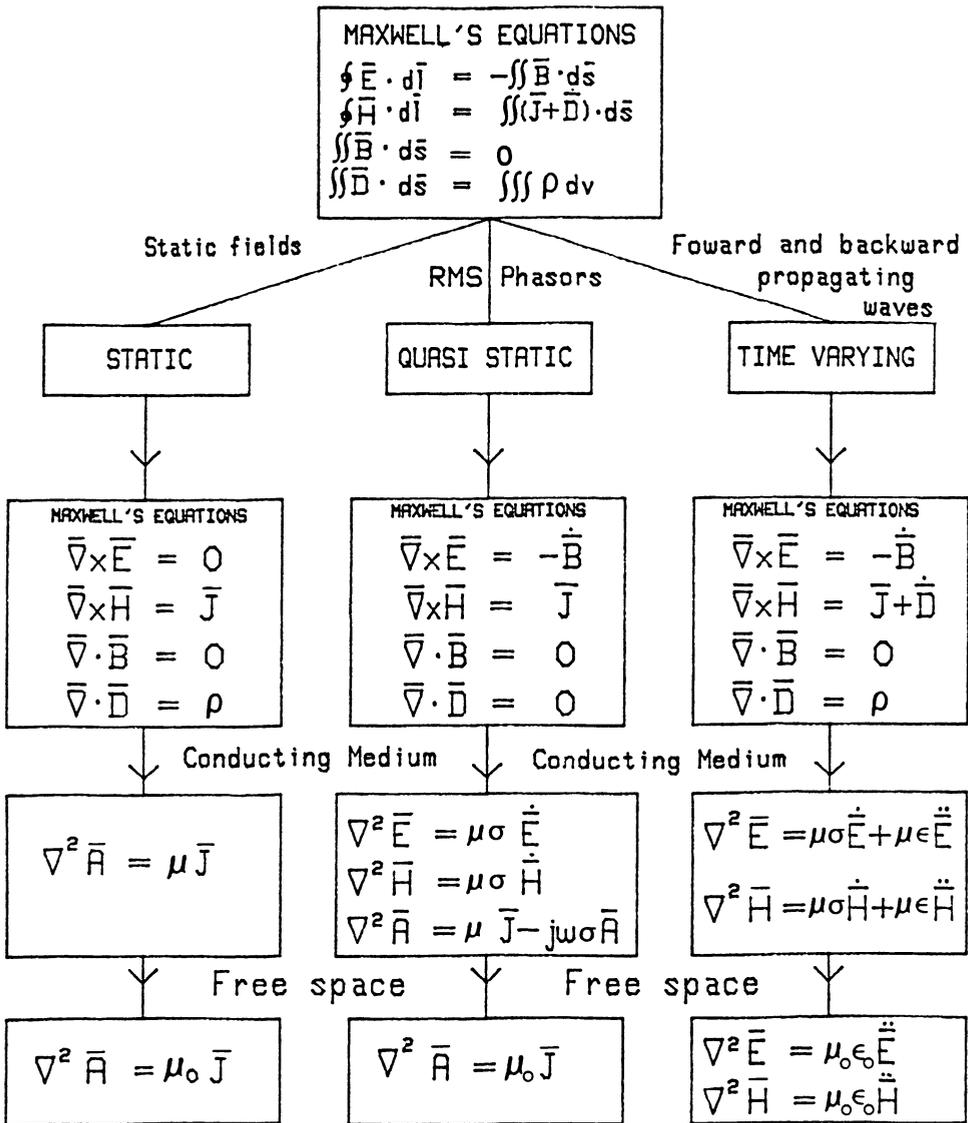
Fig. 1. Overview of Maxwell's equation in different frequency regimes.

Conventional eddy current NDT phenomena are truly steady-state alternating-current induction phenomena completely describable by quasi-static field theory. The following sections of this paper expand on these comments and discuss their implications for eddy current imaging.

PRINCIPLES OF EDDY CURRENT TESTING

As stated in the introduction, the eddy current method of nondestructive testing is principally based on Faraday's law of electromagnetic induction. When a coil excited by an alternating current source is brought close to a conducting material, the primary field set up by the coil induces eddy currents in the material, setting up an opposing, secondary field. In a nonmagnetic test object, this results in a reduction of the net flux linkages of the coil, thereby reducing the inductance of the coil. The resistance measured at the terminals of the coil is also altered to account for the eddy current losses within the material. The presence of a defect or inhomogeneity in the material causes a redistribution of the eddy currents, thereby changing the complex impedance of the probe coil. Changes in the coil impedance caused by defects in the material are represented as trajectories in the impedance plane and used for defect characterization.

From considerations of the operating frequencies and dimensions of the experimental set-up, the eddy currents constitute a quasi-static phenomenon. Under these conditions the displacement current is neglected and Maxwell's equations are

$$\bar{\nabla} \times \bar{E} = - \frac{\partial \bar{B}}{\partial t} \tag{1}$$

$$\bar{\nabla} \times \bar{H} = \bar{J} \tag{2}$$

$$\bar{\nabla} \cdot \bar{B} = 0 \tag{3}$$

$$\bar{\nabla} \cdot \bar{D} = 0 \tag{4}$$

Assuming a linear, isotropic and homogeneous medium the constitutive relations are

$$\bar{B} = \mu \bar{H} \tag{5}$$

$$\bar{D} = \varepsilon \bar{E} \tag{6}$$

$$\bar{J} = \sigma \bar{E} \tag{7}$$

Decoupling equations (1) and (2) using the constitutive relations, the governing equations for the fields and currents are

$$\nabla^2 \bar{E} = \mu\sigma \frac{\partial \bar{E}}{\partial t} \tag{8}$$

$$\nabla^2 \bar{H} = \mu\sigma \frac{\partial \bar{H}}{\partial t} \cdot \tag{9}$$

$$\nabla^2 \bar{J} = \mu\sigma \frac{\partial \bar{J}}{\partial t} \tag{10}$$

For single frequency sinusoidal excitation, the one-dimensional form of (10) can be written in the phasor form as

$$\frac{d^2\bar{J}}{dx^2} = j\omega\mu\sigma\bar{J} \tag{11}$$

The steady, state solution for the case of a sheet of alternating current density at the surface of a semi-infinite medium is given by

$$\bar{J}(x,t) = \bar{J}(0,t)\exp(-\frac{x}{\delta})\exp\{-j(\frac{x}{\delta} - \omega t)\} \tag{12}$$

where the skin depth δ is given by

$$\delta = (\frac{2}{\omega\mu\sigma})^{1/2} \tag{13}$$

Though equation (12) has the mathematical properties of an attenuated wave it does not describe a true physical wave. What it actually describes is the distribution of steady state alternating currents whose magnitude decays exponentially and whose phase angle varies linearly with depth according to the relations

$$J(x) = J(0)\ e^{-x/\delta} \tag{14}$$

$$\theta(x) = (\frac{\omega\mu\sigma}{2})^{1/2}x \tag{15}$$

Equations (12) − (15) are derived for a rather contrived geometry for the sake of computational ease. The eddy current paths in an actual eddy current test are far more complex and the presence of anomalies in the medium further perturb this distribution. However the solutions obtained above do serve to illustrate the general behavior of fields and currents and the associated skin depth which is of significant importance in eddy current NDT situations.

The phase and magnitude described above for a prescribed depth are not experimentally measurable. What is measured in an eddy current test is the complex impedance of the probe coil, which is affected by the total eddy current distribution in the test specimen.

The measured impedance of the coil can be expressed as

$$\bar{z}_c = \frac{\bar{V}}{\bar{I}} = R_c + jX_c = |z_c| \angle \phi_c \tag{16}$$

where $\bar{V}$ and $\bar{I}$ are RMS valued voltage and current phasors.

The phase angle of the eddy current test data is then given by

$$\phi_c = \text{Tan}^{-1}(\frac{X_c}{R_c}) \tag{17}$$

which does not have a simple, direct relationship with the θ of equation (15).

The eddy current test can be compared to the operation of a
transformer where the probe coil is the primary and the test material
constitutes the secondary. Just as in a transformer, the secondary pro-
perties are referred to the primary side and hence the material charac-
teristics are reflected in the coil impedance measurement. However this
measurement reveals nothing about the actual current distribution within
the test specimen. Determination of material characterstics on the
basis of the test signal from the eddy current probe is therefore a com-
plex process.

IMAGING

Imaging or inversion of eddy current data is the problem of recon-
struction of the defect in three dimensions, given the measured signal.
A direct approach by use of a theoretical model based on the underlying
physical process is too complex and most of the existing defect charac-
terization schemes resort to the indirect algorithmic methods which
depend on characteristic features in the signal for classification
information.

HOLOGRAPHIC IMAGING

In an attempt to directly image the defect in three dimensions,
Hildebrand et al.[2] apply holographic principles to eddy current data,
interpreting the eddy current phenomenon as an interference between
incident and reflected electromagnetic waves. The magnitude and phase
of the coil impedance data in (16) are thus interpreted as the magnitude
and phase of a scattered wavefront that satisfies the Helmholtz wave
equation. The method then applies a backward wave propagation[2] algo-
rithm to the eddy current data to reconstruct the defect in three dimen-
sions.

This procedure gives meaningful results only if the data input to
it indeed describes a true wave. Otherwise, the method functions as a
low pass filter with a phase response given by

$[\frac{2\pi}{\lambda} \{1-(\lambda u)^2-(\lambda v)^2\}^{1/2} z]$ which merely distorts the eddy current
probe signals.

ALGORITHMIC IMAGING

Algorithmic imaging is a procedure for deducing defect geometry
parameters by using distinctive properties of the measured signal. The
algorithmic methods for characterizing and sizing defects include signal
processing techniques such as adaptive learning networks[7], and the use
of Fourier descriptors developed by Udpa and Lord[8]. In all these
methods, the eddy current probe signals are treated as signatures of the
defect that produced them. The signal from each defect type is then
represented by a set of features either from the time domain or fre-
quency domain or a combination of both. A data bank of feature vectors
corresponding to all the expected defect types is thus built. An unk-
nown signal is then classified as belonging to one of the sets in the
data base by pattern recognition techniques.

A more direct approach has been used by Copley[9] where the phase and amplitude of the measured signal are directly interpreted in terms of defect dimensions by use of a set of calibration curves.

For the sake of comparing the results of holographic imaging and algorithmic imaging a simple image processing algorithm was implemented. Using the experimental set up shown in Figure 2, the horizontal and vertical channels of the complex probe data were sampled at discrete spatial points digitized and stored on the VAX 11/780 computer. The aluminum bar containing defect patterns such as that shown in Figure 3 was used as the test specimen. Scanning was done on the other side of bar, so that these 90% through-wall holes served as subsurface defects. In Figure 4 the complex data is displayed as four different grey-level coded images representing vertical channel data, horizontal channel data, magnitude and phase. The result of holographic imaging is shown in Figure 5 where the probe data is 'back propagated' to the plane of the defect. The result of a basic thresholding and edge detection algorithm is shown in Figure 6. This algorithm also computes the diameters of the holes. Space limitations preclude a complete discussion of all the test results comparing holographic and algorithmic imaging results. The reader is left to draw his own conclusions from Figures 5 and 6.

CONCLUSIONS

Holographic imaging algorithms can certainly be applied to the analysis of conventional eddy current probe data. The key questions highlighted by this paper are:

1.   Does such a procedure make any physical sense?

2.   Does such a procedure have distinct advantages over algorithmic imaging?

In answer, eddy current phenomena are quasi-static phenomena where the operating frequencies and characteristic dimensions are such that the displacement current is negligible. Consequently the eddy currents are described by diffusing phasors rather than by attenuated waves. Secondly, in an eddy current test the measured probe impedance is caused by the integrated effect of all the currents in the specimen and hence the phase of the test data cannot represent the phase of induced eddy currents or the phase of an electromagnetic wave. Thus the indirect nature of the eddy current test makes a direct approach to the inverse problem very complex and algorithmic methods appear to be a more practical solution.

ACKNOWLEDGMENTS
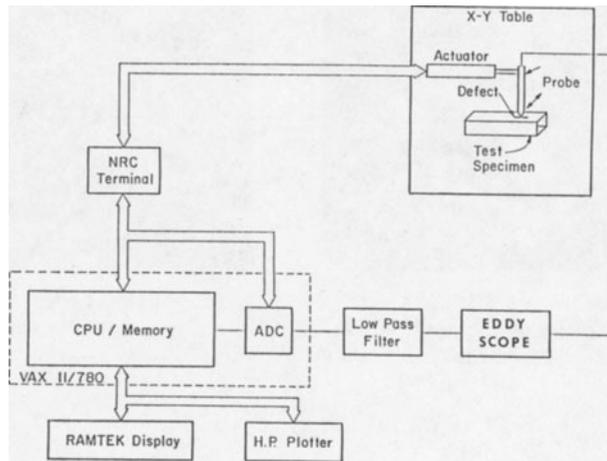
Fig. 2.   Data acquisition system.
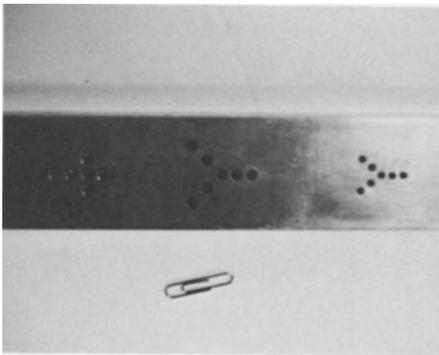

Fig. 3.   Al bar with defect
          patterns.
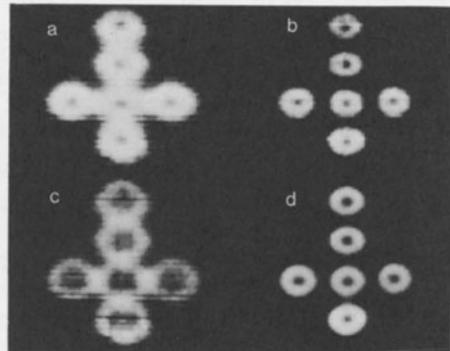

Fig. 4.   Images of a) horizontal
          channel, b) vertical channel,
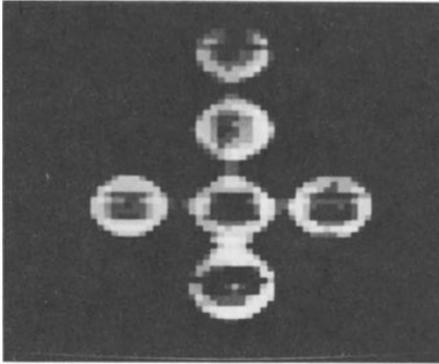   c) magnitude, d) phase of
          eddy current data.

Fig. 5.   Results of holographic
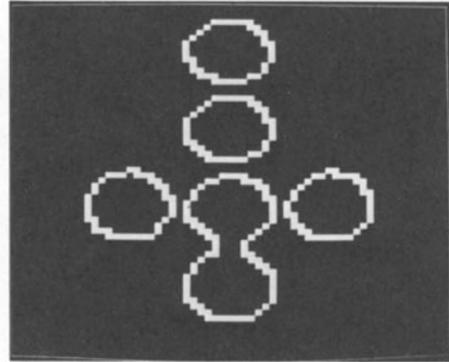   imaging using magnitude
          and phase data.

Fig. 6.   Results of an edge detection
          algorithm on Fig. 4d.

REFERENCES

1.   D. E. Hughes, Induction-balance and experimental researchers
     therewith, Phil. Mag. 8:50 (1879).

2.   B. P. Hildebrand and G. L. Fitzpatrick, Inversion of eddy current
     data using holographic principles, Review of Progress in Quantita-
     tive NDE, La Jolla, 1984.

3.   R. Hochschild, Electromagnetic methods of testing metals, in "Pro-
     gress in non-destructive testing," Vol. 1, E. G. Stanford et al.,
     Macmillan, New York, 1959.

4.   R. L. Stoll, "The Analysis of Eddy Currents," Oxford University
     Press, 1974.

5.   R. L. Ferrari, "An Introduction to Electromagnetic Fields," Van
     Nostrand Reinhold, New York, 1975.

6.   J. R. Melcher and H. H. Woodson, "Electromechanical Dynamics,"
     Part I, Wiley, New York, 1968.

7.   A. G. Ivakhnenko, The group method of data handling − a rival of the
     method of stochastic approximation, Soviet Automatic Control, 13:43
     (1968).

8.   S. S. Udpa and W. Lord, A Fourier descriptor classification scheme
     for differential probe signals, Materials Evaluation, 42:1136
     (1984).

9.   D. C. Copley, Eddy current imaging for defect characterization, in
     "Review of Progress in Quantitative Nondestructive Evaluation," D.
     Thompson and D. Chimenti eds., Plenum, New York (1984).